RESEARCH ARTICLE

Synergistic topological and supramolecular control of Diels-Alder reactivity based on a tunable self-complexing host-guest molecular switch

Cédric Ribeiro,[a] Michele Cariello,[b] Aurélie Malfait,[a] Marc Bria,[a] David Fournier,[a] Joël Lyskawa,[a] Gaëlle Le Fer,[a] Jonathan Potier,[a] Richard Hoogenboom,*[c] Graeme Cooke,*[b] Patrice Woisel*[a]

[a] C. Ribeiro, A. Malfait, M. Bria, Dr D. Fournier, Prof J. Lyskawa, Dr G. Le Fer, Dr J. Potier, and Prof P. Woisel*[a]
Univ. Lille, CNRS, INRAE, Centrale Lille, UMR 8207 - UMET - Unité Matériaux et Transformations
F-59000 Lille (France)
E-mail: patrice.woisel@centralelille.fr

[b] Dr Michele Cariello and Prof. G. Cooke
School of Chemistry,
University of Glasgow
Glasgow, G12 8QQ (United Kingdom)
E-mail: Graeme.Cooke@glasgow.ac.uk

[c] Dr. V.R. de la Rosa, Prof. R. Hoogenboom
Supramolecular Chemistry Group, Department of Organic and Macromolecular Chemistry
Ghent University
Krijgslaan 281 S4-bis, 9000 Ghent (Belgium)
E-mail: Richard.hoogenboom@ugent.be

These authors contributed equally

Abstract: Compartmentalization and binding-triggered conformational change regulate many metabolic processes in living matter. Here, we have synergistically combined these two biorelevant processes to tune the Diels-Alder (DA) reactivity of a synthetic self-complexing host-guest molecular switch **CBPQT^{4+}-Fu**, consisting of an electron-rich furan unit covalently attached to the electron-deficient cyclobis(paraquat-p-phenylene) tetrachloride (**CBPQT^{4+}, 4Cl-**) host. This design allows **CBPQT^{4+}-Fu** to efficiently compartmentalize the furan ring inside its host cavity in water, thereby protecting it from the DA reaction with maleimide. Remarkably, the self-complexed **CBPQT^{4+}-Fu** can undergo a conformational change through intramolecular decomplexation upon the addition of a stronger binding molecular naphthalene derivative as a competitive guest, triggering the DA reaction upon addition of a chemical regulator. Remarkably, connecting the guest to a thermoresponsive lower critical solution temperature (LCST) copolymer regulator controls the DA reaction on command upon heating and cooling the reaction media beyond and below the cloud point temperature of the copolymer, representing a rare example of decreased reactivity upon increasing temperature. Altogether, this work opens up new avenues towards combined topological and supramolecular control over reactivity in synthetic constructs, enabling control over reactivity through molecular regulators or even mild temperature variations.

Introduction

The compartmentalization of (bio)chemical functions is a central feature of living matter.[1,2] Biological systems can physically and spatially confine molecular constituents and functions in delimited compartments through thermodynamic and/or kinetic barriers while enabling molecular communication and energy exchange with their external environments to regulate vital biochemical processes.[3,4] One typical example is the compartmentalized nucleus of eukaryotic cells that acts as a biological host to store the genetic material and regulate the DNA transcription by guiding the chromosome folding in the nuclear space through spatial interactions.[5–7] Other fascinating compartmentalized natural hosts are viral capsids composed of several self-assembled oligomeric proteins that package and protect genomic material, infect other host organisms, and quickly open up to release the genome after replication.[8,9] Over the years, inspired by such biological systems, many scientists have designed synthetic host structures that mimic the functionality achieved by compartmentalized natural systems. Hence, various synthetic capsules have been reported to efficiently sequester guests (*i.e.,* with high affinity and selectivity) and modulate their reactivity.[10,11] According to the design of host-guest systems, the reactivity of guests can be exacerbated with potentially an enhancement of selectivity, or conversely, capsule cavities can act as protective vessels from external environments or events, allowing the stabilization of short-lived guests or metastable intermediates.[12–17] In this context, the Diels-Alder (DA) cycloaddition reaction,[18] which counts as one of the most popular transformations in Organic Chemistry, has often been used as a model reaction to illustrate the ability of synthetic host systems to drive the course of a chemical reaction in terms of kinetics and selectivity of adducts when carried out in water with suitable supramolecular receptors. In this vein, Fujita and co-workers have engineered self-assembled coordinated cages[19,20] and porous networks[21,22] that can trap DA substrates (dienes and dienophiles) through intermolecular interactions and mediate DA reactions of

unreactive dienes and/or cycloadditions with enhanced reactivity and controlled regioselectivity. Furthermore, computational methods were undertaken for the *de novo* design of an enzyme that catalyzes the DA reaction with high stereoselectivity and substrate specificity.[23] Scherman and co-workers also reported the use of the Cucurbit[7]uril host (CB[7]) as a supramolecular artificial enzyme to perform intramolecular DA cycloaddition reactions of unreactive *N*-allyl-2-furfurylamine derivatives in an aqueous environment.[24] Upon complexation with CB[7], a rearrangement of substrates occurs within the host cavity, leading to a highly reactive conformation resulting in asymmetric cycloadditions. Recently, Nitschke and co-workers also showed that iron-based coordinated cages could encapsulate furan and serve as protecting environment, impeding its reaction with maleimide in water.[25]The entrapped furan could be released upon adding a competing guest as a regulator to switch on the DA reaction.

Besides compartmentalization capability, biological systems are also intrinsically dynamic, and this peculiar characteristic significantly affects their function. For instance, proteins can feature significant ligand-induced conformational changes.[26–28] These conformational changes can have topological effects that result in the release or the blocking of reactive sites of the protein and thus regulation of the biological function, including catalysis,[29,30] signaling,[31] and self-assembly of biomacromolecules into complex architectures[32] for therapeutic applications.[33,34]

Here, we combined the two concepts, *i.e.*, compartmentalization and regulator-induced conformational change, to control the Diels-Alder reactivity between a furan moiety and maleimide in water. In particular, we have designed a furan functionalized cyclobis(paraquat-*p*-phenylene) tetrachloride ($CBPQT^{4+}$,$4Cl^-$) **$CBPQT^{4+}$-Fu** derivative where the electron-rich cyclic diene unit formed a stable self-complexed conformation with the $CBPQT^{4+}$ moiety in water as shown in Figure 1. This closed intramolecularly complexed topology compartmentalizes the furan sub-unit inside the host cavity, thereby preventing its reaction towards maleimide in water. Nevertheless, upon adding naphthalene derivatives (**Napht-1** and **Napht-2**) as regulators with a higher binding affinity towards the $CBPQT^{4+}$ host compared to the furan unit, the **$CBPQT^{4+}$-Fu** will adopt a new open conformation where the furan unit is located outside the protective host cavity, enabling the DA reaction with maleimide, resulting in the initiation of the DA process. Increasing the temperature of an organic reaction generally speeds up its rate. Here, conversely, we demonstrate that the combined topological and supramolecular control enables us to switch off the DA at high temperature, while it is enabled by lowering the temperature. This has been achieved by using a thermoresponsive naphthalene end-functionalized copolymer **Napht-2** displaying a cloud point (T_{cp}) in water as thermoresponsive regulator for the DA reactivity[35]. The thermoresponsive copolymer regulator could be easily removed from the reaction after the DA transformation, leading to the uncomplexed cycloadducts of **$CBPQT^{4+}$-Fu** and maleimide. The designed molecular system and regulators are shown in **Figure 1**.

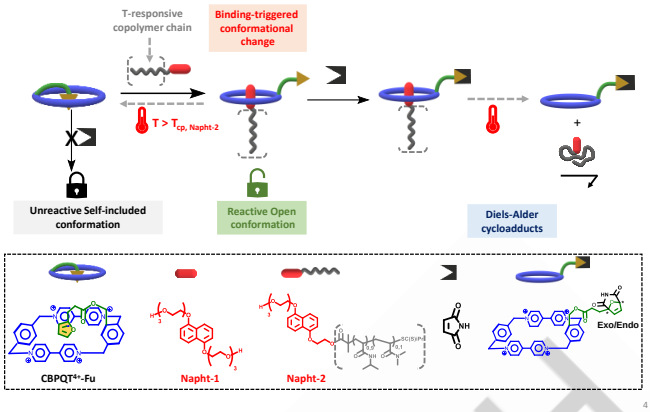

Figure 1. Principle of the control over Diels-Alder reactivity based on a tunable self-complexing host-guest molecular switch **$CBPQT^{4+}$-Fu**. Molecular structures of **$CBPQT^{4+}$-Fu** (Cl^- counterions not included), **Napht-1** and **Napht-2** guestsMain Text Paragraph.

Results and Discussion

$CBPQT^{4+}$-Fu was synthesized from the dipyridinum salt 1[36] and the dibromobenzyl derivative 2[37] through the template-directed clipping methodology, using an electron-rich naphthalene based template (Figure 2A; experimental details are provided in the Supporting Information). After the reaction, the template was removed by liquid-liquid extraction ($CHCl_3/H_2O$) and the pure $CBPQT^{4+}$-Fu was obtained as a deep yellow solid in 30 % yield following silica column chromatography.

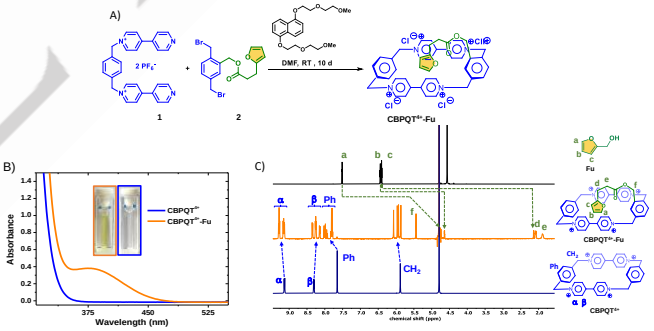

Figure 2. A) Synthetic route for **$CBPQT^{4+}$-Fu** starting from **1** and **2**; B) UV-visible spectra of **$CBPQT^{4+}$** and **$CBPQT^{4+}$-Fu**, recorded in water at 25°C; C) ^{1}H NMR spectra of **Fu** (top), **$CBPQT^{4+}$-Fu** (middle) and **$CBPQT^{4+}$**(down) recorded in D_2O at 25°C.

The optical absorption of the complex in the visible light region arises from the formation of a donor-acceptor charge-transfer (CT) interaction between the electron-rich furan moiety and the electron-deficient $CBPQT^{4+}$ cavity, and was confirmed by the absorption band centered at 380 nm in the UV-Vis spectrum of $CBPQT^{4+}$-Fu in water (Figure 2B). ^{1}H NMR spectroscopy (Figure 2C) provided further evidence for the furan moiety being accommodated inside the host cavity. A clear deshielding (+0.2 ppm<$\Delta\delta$<+0.4 ppm) for H_α and H_{Ph} protons on the $CBPQT^{4+}$ macrocycle was also observed, whereas all protons belonging to the guest moiety experienced shielding ($\Delta\delta_{Ha}$= -2.8 ppm, $\Delta\delta_{Hb}$= -1.8 ppm, $\Delta\delta_{Hc}$= -4.3 ppm) compared with those for the free Fu. The large magnitude of these upfield shifts of the furan protons during the complexation indicates that they are engaged in

addition to π–π interactions with the bipyridinium segments, and strong edge-to-face C-H-π interactions with the *p*-phenylene linkers in the ring, which is consistent with previously reported Naphthalene:CBPQT^{4+} based complexes.[38] This proximity of the protons mentioned above in the complex was confirmed in the 2D NOESY spectrum (Supporting Information, Figure S15), which revealed notably strong cross-correlations between the H_a, H_b, H_c protons of the furan moiety and the H_α, H_β, and H_{Ph} protons of the cyclophane part, and between the H_β and the methylene protons H_d, H_e of the linker of CBPQT^{4+}-Fu, suggesting that the furan moiety adopts a near central and deep position inside the cavity.

Concentration dependence (studied concentration ranges up to 50 mM) was not observed in the proton resonances in the NMR spectra, and furthermore, the diffusion coefficient (D) of protons belonging to **CBPQT^{4+}-Fu**, and the heat exchange from isothermal titration calorimetry (ITC) experiments (Supporting Information, Figure S16 and S17),[39] provided evidence for an intramolecular self-included conformation for **CBPQT^{4+}-Fu**. ITC titration experiments between **CBPQT^{4+}-Fu** and a strong binding naphthalene guest (**Napht-1**)[40] were also undertaken to evaluate the equilibrium constant K_{in} (Figure 3),[41] defined as the concentration ratio **[CBPQT^{4+}-Fu-in]/ [CBPQT^{4+}-Fu-out]**, and the apparent association constant K_{app} related to **CBPQT^{4+}-Fu-in/ CBPQT^{4+}-Fu-out**:**Napht-1** complexes (Supporting Information, Table S1 and Figure S18). Thermodynamic data exhibited no significant difference in association strength between **Napht-1** and both **CBPQT^{4+}** (K_a=8.6 ×10^5 M^{-1}) and preformed **CBPQT^{4+}:Fu** complex (K_a=9.5 ×10^5 M^{-1}), which was in line with the relatively low binding affinity of **Fu** toward **CBPQT^{4+}** (K_a =10^2 M^{-1}) determined by UV-Vis titration (Supporting Information, Figure S20). Remarkably, the **Napht-1** guest displayed a thousand times lower association constant with **CBPQT^{4+}-Fu** (K_{app} = 6.2 x 10^2 M^{-1}) than **CBPQT^{4+}**. K_{in} could be estimated to be ~1×10^3 from these binding experiments, confirming the significant prevalence of the **CBPQT^{4+}-Fu-in** form for **CBPQT^{4+}-Fu** in solution. UV-vis spectroscopy next confirmed the thermal stability of **CBPQT^{4+}-Fu-in** as spectra recorded at different temperatures (Supporting Information Figure S19) showed no significant decrease in the charge transfer absorption band centred at 380 nm at least up to 85°C. Further confirmation of the prevalent self-included conformation **CBPQT^{4+}-Fu-in** was also given through density functional theory (DFT) calculations (Figure 3, details are provided in Supporting Information).[42] Geometry-optimized structures in water revealed less twisted pyridinium rings and a smaller inter-planar distance (d) in **CBPQT^{4+}-Fu-in** (d = 3,2 Å) than in **CBPQT^{4+}-Fu-out** (d = 3,4 Å), suggesting the possible formation of π-π stacking interactions between the furan and the two viologens surrounding it for **CBPQT^{4+}-Fu-in**. This was confirmed by the electrostatic potential (ESP) maps showing a clear contrast between the more positive (blue) area inside the cavity and the more negative (red) furan unit for **CBPQT^{4+}-Fu-out**, whereas the electrostatic difference was more muted in **CBPQT^{4+}-Fu-in**, indicating that charge-transfer takes place between the guest and the host. Also in line with the experimental results is the further stabilization of the furan in **CBPQT^{4+}-Fu-in** through the formation of non-covalent CH-π interactions between the *p*-xylyl rings and H_a (2.6 Å) and H_c (3.2 Å). The conformational locking of the furan unit linked to the ring through CH-π interactions and the CT complex could also explain the higher stability of **CBPQT^{4+}-Fu-in**, which was found experimentally to be the prevalent conformer. A difference in total energy (sum of the zero point and electronic contribution) of 6.69 kcal/mol was found between the two conformations.

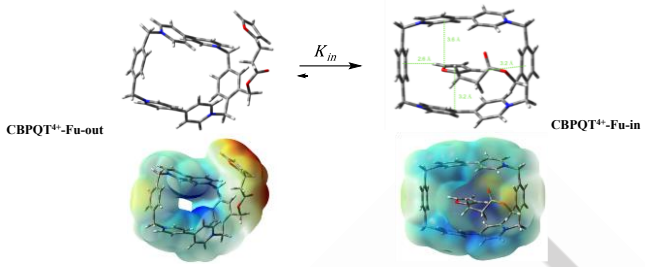

Figure 3. Thermodynamic equilibrium between **CBPQT^{4+}-Fu-out** and **CBPQT^{4+}-Fu-in**; DFT geometry optimization and ESP distribution of **CBPQT^{4+}-Fu-out** and **CBPQT^{4+}-Fu-in**.

After confirming that **CBPQT^{4+}-Fu** formed a stable self-inclusion complex, we next examined the chemical reactivity of its furan moiety with maleimide at 25°C in water. Therefore, we monitored the formation of DA cycloadducts (*exo* and *endo* isomers) in the presence of an excess of maleimide (16-fold excess, *i.e.*, under pseudo-first-order kinetic conditions) by in situ ^{1}H NMR spectroscopy (Supporting Information, Figure S27). As control experiments, the kinetics of DA reactions were also recorded for **Fu** and the intramolecular **CBPQT^{4+}:Fu** complex in similar conditions with an excess of maleimide (Supporting Information, Figure S23 and S25). The progress of the DA reactions of **Fu**, **CBPQT^{4+}:Fu**, and **CBPQT^{4+}-Fu** with maleimide, shown in Figure 4A, shows similar trends for both cycloadditions with a complete conversion reached after 1200 minutes and comparable pseudo-first-order reaction rate constants (k_1, k_2) of ~3×10^{-3} min^{-1} (Figure 4B). This observation agrees with the relatively low association constant and the dynamic nature of the **CBPQT^{4+}:Fu** complex as determined by UV-Vis and NMR spectroscopy, respectively (Supporting Information, Figure S21).

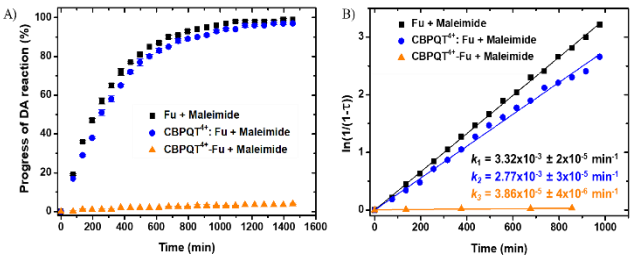

Figure 4. A) Diels-alder reaction kinetics at 25°C in water between maleimide (16 equiv.) and **Fu** (■), **CBPQT^{4+}:Fu** (●) or **CBPQT^{4+}-Fu** (▲), B) Plots of the ln(1/(1-τ)) vs time in the DA reaction of maleimide with **Fu** (■), **CBPQT^{4+}:Fu** (●), or **CBPQT^{4+}-Fu** (▲). τ is the conversion for the formation of cycloadducts. The pseudo-first-order rate constants (k_1, k_2, k_3) were obtained from the slopes of the pseudo-first kinetic plots.

Remarkably, the kinetic study relating to the DA reaction of **CBPQT^{4+}-Fu** with maleimide revealed a negligible conversion of its furan moiety into corresponding cycloadducts with the studied time-frame, and an extremely low pseudo-first-order reaction rate constant (k_3), that is 100 times lower compared to the model reactions, thereby univocally demonstrating that the synergistic topological and supramolecular effects suppress the DA reactivity

of the furan-moiety of **CBPQT^{4+}-Fu**. DFT investigations provided theoretical insights into the molecular reactivity of **CBPQT^{4+}-Fu-in** towards a DA reaction with a dienophile (*e.g.,* maleimide) (Supporting information Figure S22). These calculations indicated i) that the highest occupied molecular orbital (HOMO) was localised on the furan, whereas the lowest unoccupied molecular orbital (LUMO) was delocalized over the viologen units, and ii) the proximity of furan and viologen in **CBPQT^{4+}-Fu-in** induced the overlap of the frontier molecular orbital and the formation of the intra-molecular CT complex, thus preventing the spatial overlap between the HOMO of the furan and the LUMO of the dienophile. Hence, the lack of the reactivity of **CBPQT^{4+}-Fu-in** would have a dual origin: the steric hindrance conferred by the tetracationic macrocycle and the electronic deactivation of the furan moiety towards undertaking DA reaction.

We have previously shown that **Napht-1** can bind **CBPQT^{4+}-Fu** through ITC experiments. To probe whether the intermolecular **Napht-1:CBPQT^{4+}-Fu** complex formation could result in a conformational change of **CBPQT^{4+}-Fu** (from **CBPQT^{4+}-Fu-in** to **CBPQT^{4+}-Fu-out**), UV-vis and ^{1}H NMR spectroscopic titrations were carried out. Upon addition of aliquots of **Napht-1** to a **CBPQT^{4+}-Fu** solution, UV-visible spectra (Supporting Information Figure S37) showed the disappearance of the absorption band of the self-complexed **CBPQT^{4+}-Fu** (at λ=380 nm) and the simultaneous emergence of an absorption at λ= 520 nm due to the intramolecular **Napht-1 :CBPQT^{4+}-Fu** complex.[43] The ^{1}H NMR spectra (Supporting Information Figure S38) exhibited new signals for the complexed naphthalene unit ($\delta_{H2/6}$ ~ 6.5 ppm, $\delta_{H3/7}$~ 6.3 ppm, and $\delta_{H4/8}$ ~ 2.9 ppm) and uncomplexed furan moiety (δ_{Ha} ~ 7.4 ppm, δ_{Hb} ~ 6.2 ppm and δ_{Hc} ~ 6.1 ppm), respectively, accompanied by the disappearance of resonance of H_b and H_c protons in its complexed form. Thus, these results confirmed the ousting of the furan from the cyclophane ring upon the addition of **Napht-1**. Hence, **Napht-1** acts as a topological regulator by inducing the release of the furan moiety.

We then investigated whether this conformational change of **CBPQT^{4+}-Fu**, when exposed to **Napht-1**, could initiate the DA reaction between the non-complexed Fu and the maleimide. Indeed, the DA kinetics confirmed that the addition of **Napht-1** as a regulator released the reactivity of the furan moiety, which showed similar conversion (Figure 5A) and kinetic rate (Figure 5B) for the DA reaction with maleimide as the model system (*i.e.,* DA between **Fu** and maleimide).

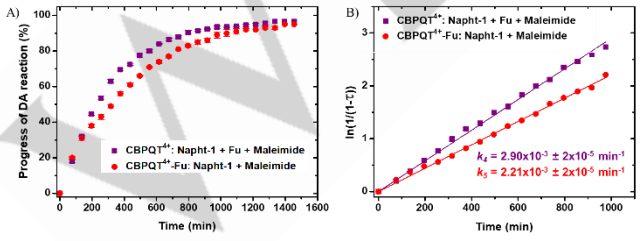

Figure 5. A) Diels-alder reaction kinetics at 25°C in water between maleimide (16 equiv.) and **CBPQT^{4+}:Fu** (■)or **CBPQT^{4+}-Fu** (●), B) Plots of the ln (1/(1-τ)) vs time in the DA reaction of maleimide with **CBPQT^{4+}:Fu** (■) or **CBPQT^{4+}-Fu** (●). □ is the conversion for the formation of cycloadducts. The pseudo-first-order rate constants (k_3, k_4) were obtained from the slopes of the pseudo-first kinetic plots.

Previously, we reported the switch on/off regulation of the recognition properties of **CBPQT^{4+}** in aqueous media through the coil-to-globule transition (LCST) of thermosensitive (co)polymers featuring complementary naphthalene guest modules.[35,44] In such systems, a full disassembly of the complexes was observed upon heating the solutions above their T_{cp}, leading to the precipitation of Naphthalene functionalized co(polymers) and the liberation of free host **CBPQT^{4+}** into the solution. Here, we hypothesized that this thermally controlled phase transition of **Napht-2**, showing a T_{cp} of 27°C (for details regarding its synthesis and characterizations, see Supporting Information), could be used to turn on and off the DA reaction between **CBPQT^{4+}-Fu** and maleimide at low ($T<T_{cp}$) and high ($T>T_{cp}$) temperature, respectively. As a control experiment, we first investigated the influence of temperature on the progress of the DA reaction between the **Napht-1/CBPQT^{4+}-Fu$_{out}$** complex and maleimide. As reported for other DA reactions [45], the conversion was in line with the Arrhenius equation and proceeded more quickly when the temperature raised from 25 to 45°C (see Supporting Information Figure S39 and S40).

Figure 6 shows the progress of the Diels-Alder reaction in the presence of **Napht-2** at different temperatures. At 25°C (below T_{cp}), the sample was purple due to complex formation between **Napht-2** and **CBPQT^{4+}-Fu,** and the DA reaction proceeded as the furan moiety was outside the CBPQT^{4+} cavity. At a temperature above T_{cp}, the sample lost its purple color (indicating the decomplexation of the **Napht-2:CBPQT^{4+}-Fu** complex) and became turbid (due to the collapse of the **Napht-2)**. A UV-vis spectrum recorded on **Napht-2/ CBPQT^{4+}-Fu$_{out}$** at 45°C confirmed its dissociation above the T_{cp}, and the concomitant reformation of the self-included **BB-F$_{in}$** conformation by the disappearance of the characteristic absorption band at 520 nm and the re-emergence of an absorption at 380 nm, respectively (see Supporting Information Figure S42). Importantly, in contrast to the DA reaction between carried out lower temperatures, the DA reaction stopped at elevated temperature, and no conversion of the furan sub-unit was observed, confirming the LCST-induced control over the DA reaction between **CBPQT^{4+}-Fu** and maleimide. Furthermore, no retro-DA reactions were observed at 45°C, indicating the thermal stability of cycloadducts in conditions used for kinetic investigations (see Supporting Information Figure S44). Finally, upon re-cooling the sample below the T_{cp}, the DA reaction restarted due to the re-solubilization of the copolymer and its subsequent complexation with **CBPQT^{4+}-Fu** to finally reach 100% conversion. Furthermore, once fully converted, cycloadducts can be isolated from **Napht-2** by a simple workup, including a filtration step at $T>T_{cp}$ (see details in Supporting Information).

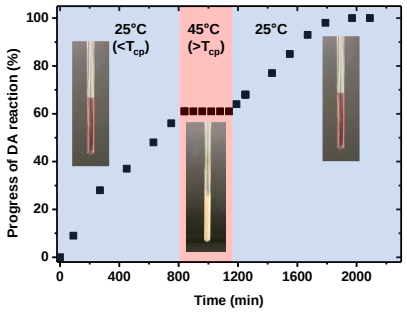

Figure 6. Diels-Alder reaction kinetics at 25°C in water between maleimide (16 equiv.) and **CBPQT^{4+}-Fu** (■) in the presence of the thermoresponsive **Napht-2** (3 equivalent) as a guest, under different heating regimes (T=25°C for 800 minutes followed by T=45°C for 300 minutes and finally T=25°C for 1000 minutes). Photographs show changes in color and phase transitions of the

sample containing **CBPQT^{4+}-Fu, Napht-2,** and maleimide during the heating treatment.

Conclusion

In summary, we have successfully demonstrated the synergistic control over furan DA reactivity through supramolecular association and topological effects by coupling the furan to CBPQT^{4+}. Within this system, the cyclic diene subunit was efficiently compartmentalized inside the host moiety, masking its reactivity towards a DA reaction with maleimide. Adding more strongly binding naphthalene guest molecules as topological supramolecular regulators resulted in the release of the furan guest subunit from the protective host vessel, thereby triggering the DA reaction between furan and maleimide. This molecularly controlled regulation of furan reactivity was subsequently transformed into a temperature-induced control of the DA reactivity through the coil-to-globule transition (LCST) of a thermosensitive naphthalene end-functionalized (co)polymer. As such, the reactivity of the furan moiety could be switched on at lower temperatures (below the T_{cp}) while it was switched off at elevated temperatures (above T_{cp}), representing a rare example of lower reactivity at raised temperature. This work provides thus essential insight into synergistically controlling chemical reactivity through supramolecular topological chemistry, combined with different regulators (molecular and thermal), providing an important step towards synthetic molecular reaction networks.

Experimental Section

Materials

Unless otherwise stated, commercially available materials were used without purification. *N*-Isopropylacrylamide (NIPAm, ≥ 98 %, Aldrich) was recrystallized from *n*-hexane and 2,2′-azobis(isobutyronitrile) (AIBN, ≥ 98 %, Aldrich) was recrystallized from methanol. *N,N*-Dimethylacrylamide (99 %, Aldrich) was passed through basic aluminum oxide column to remove the inhibitor before use. All organic solvents were analytical grade and water was purified with a Millipore system combining inverse osmosis membrane (Milli RO) and ion exchange resins (Milli Q) for purification.

NMR spectroscopy

^{1}H, ^{13}C, COSY ^{1}H-^{1}H and HSQC ^{1}H-^{13}C NMR spectra were recorded on a Bruker 300 MHz AVANCE III HD spectrometer using a standard 5mm BBFO Probe at 25 °C. Deuterated acetonitrile (CD_3CN) and deuterated water (D_2O) were used as solvents and all chemical shifts (δ) were expressed in ppm relative to the residual solvent protons. Coupling constants (J) are reported in Hz and relative intensities are reported. Two-dimensional diffusion-ordered ^{1}H NMR spectroscopy (DOSY) experiments were performed at 25 °C on a Bruker AVANCE NEO spectrometer operating at 400 MHz (9.4 T) using a 5 mm TBI Probe and equipped with a Bruker multinuclear z-gradient inverse probe head capable of producing gradients in the z direction with strength of 5.35 G.mm^{-1}. The DOSY spectra were acquired with the ledbpgp2s pulse program from Bruker Topspin software. All spectra were recorded with 16,384 time-domain data points in t_2 dimension and 16 t_1 increments. The gradient strength was logarithmically incremented in 16 steps from 2 % up to 95 % of the maximum gradient strength. All analyses were performed with a compromise diffusion delay Δ of 0.06 s in order to keep the relaxation contribution to the signal attenuation constant for all samples. The gradient pulse length δ was 2100 µs in order to ensure full signal attenuation. The D1 value was 10 s. The diffusion dimension of the 2D DOSY spectra was operating by DOSY treatment software Bruker Topspin 4.1.4 and Dynamics center version 2.8.0.1. 2D NMR nuclear Overhauser enhancement spectroscopy (NOESY) were performed at 25 °C and acquired at 400 MHz, using a 650 ms mixing time and a 10 µs ^{1}H 90° pulse width. The experiments were done with 256 numbers of experiments (TD F1), 4 numbers of scan (NS) and 10.773 W power level for pulse (PlW1).

For the kinetic investigation of the Diels-Alder reactions, ^{1}H NMR spectra were recorded on a Bruker AVANCE NEO spectrometer at 400 MHz and at 25 °C with the following experimental conditions: 128 scans, 2 s relaxation delay and 6.5 µs pre-scan delay. Concerning the kinetic monitoring of the Diels-Alder reaction in presence of **Napht-2** copolymer, ^{1}H NMR spectra were recorded on a Bruker AVANCE NEO spectrometer at 400 MHz at 45 °C (precipitated state) and at 25 °C (soluble state) with the following experimental conditions: 128 scans, 2 s relaxation delay and 6.5 µs pre-scan delay.

Fourier transform infrared (FTIR) spectroscopy

FTIR spectra were registered on a Perkin Elmer Spectrum Two equipped with an attenuated total reflection (ATR) accessory. The spectra were recorded in a range of 450-4000 cm^{-1}, a resolution of 4 cm^{-1} and 16 scans were performed for each specimen.

UV-vis spectroscopy

An Agilent Cary 3500 Scan UV-Visible spectrophotometer equipped with a multicell Peltier temperature controller was used. For the variable-temperature investigations, a solution of **CBPQT^{4+}-Fu** was prepared at 1.5 mM and placed in a 10 mm path length quartz cell. For all titration experiments, UV-Visible spectra were recorded at 20 °C. A 12 mM solution of **Napht-2** copolymer was prepared and placed in a 10 mm path length quartz cell. Turbidimetry curves were built by collecting the absorbance at 700 nm with a scanning rate of 1 °C.min^{-1}. The cloud point temperatures were determined during the heating ramp at 50 % transmittance.

Elemental analysis method description

The compounds (CHNS) were determined using the thermo scientific FlashSmart automated analyzer. For CHNS determination, the samples were weighted in tin containers and introduced into the combustion reactor. The reactor is filled with copper oxide followed by wire reduced nickel and maintained at 950°C and operates with dynamic flash combustion of the sample. The N, C, H and S were detected as N_2, CO_2, H_2O and SO_2 respectively. The resulted gases were separated on a packed column heated at 65°C in an oven and detected by a TCD (thermal conductivity detector). For each sample, 3 replicates were done

Isothermal Titration Calorimetry (ITC)

The affinity constant of **CBPQT^{4+}-Fu:Napht-1** complex was measured at 20 °C using a nano-ITC titration calorimeter from TA Instruments following standard procedures. Compounds were dissolved in Milli-Q water and the solutions were degassed gently under vacuum before use. The sample cell (~1 mL) was initially filled with **Napht-1** or Milli-Q water for dilution measurements, while **CBPQT^{4+}-Fu** solution was introduced into a 250 µL injection syringe. Each titration comprised an initial 2 µL pre-injection followed by 24 × 10 µL of **CBPQT^{4+}-Fu** solution into the sample cell under continuous stirring (400 rpm). A similar procedure was used at 20 °C for the titration of **CBPQT^{4+}** and **CBPQT^{4+}:Fu** with **Napht-1**. Control experiments with identical injections of **CBPQT^{4+}-Fu**, **CBPQT^{4+}** and **CBPQT^{4+}:Fu** into Milli-Q water were used to correct the titration baseline. The enthalpy of complexation (ΔH) was obtained after subtraction of the dilution curve from the titration one. The association constant (K_a), as well as other thermodynamic parameters including free energy (ΔG) and entropy (ΔS), were obtained after data fitting using the independent fitting model.

Size exclusion chromatography (SEC)

Size exclusion chromatography (SEC) analysis was carried out at 35 °C in DMF as mobile phase at a flow rate of 0.7 mL.min^{-1} using toluene as a flow marker. **Napht-2** copolymer solution was prepared at a concentration of 5 mg.mL^{-1} and filtered through a 0.45 µm PTFE membrane. SEC measurements were performed on a Agilent system equipped with three columns (PLgel 100A, PLgel 500A, PLgel 10E4A) placed in series and coupled with a differential refractive index (RI) detector from Wyatt (Optilab). The relative number-average molar mass ($\overline{M_n}$), relative weight-

average molar mass ($\overline{M_w}$) and the dispersity ($Đ = (\overline{M_w}/\overline{M_n})$) were calculated from a calibration curve based on narrow poly(methyl methacrylate) (PMMA) standards.

Computations

DFT calculations were run to better understand the chemical reactivity of CBPQT^{4+}-Fu towards the Diels-Alder reaction. Two configurations of the tetracationic molecule, with the furan inside (CBPQT^{4+}-Fu$_{in}$) or outside (CBPQT^{4+}-Fu$_{out}$), were geometrically optimized, using the RM062X functional with a 6311**G (d,p) basis set. A first optimization was run in vacuum, followed by a second one in water (IEFPCM). The absence of negative frequencies was verified through frequency calculations at the same level of accuracy. No imaginary frequencies were detected. Total energy were obtained as the sum zero point and electronic energies. The coordinates of the geometrically optimized molecules in water are reported in Table S2 (Supporting Information).

Synthesis

2-Hydroxymethyl furan (**Fu**) (98 %, Aldrich) was purified by distillation before use. Compounds **Napht-1**,[46], **CBPQT^{4+}**[47],**1**[49] and the naphthalene based template [50] were synthesized following literature procedures.

Compound 2. A solution of 3-(2-furyl)propionic acid (1.77 g, 12.65 mmol), 1,3-dicyclohexylcarbodiimide (2.6 g, 12.65 mmol), 4-dimethylaminopyridine (0.154 g, 1.265 mmol) and compound **1** (2.86 g, 9.73 mmol) in dry CH_2Cl_2 (200 mL) was stirred under N_2 for 48 h at room temperature. The resulting suspension was filtered and the filtrate was dried under vacuum. The residue was purified using column chromatography (SiO_2: CH_2Cl_2/petroleum ether, 4:6). All fractions containing the product were combined together and concentrated under vacuum to obtain compound **2** as a white solid (3.24 g, 7.78 mmol, 80% yield).

^{1}H NMR: (300 MHz, CD_3CN, 298 K): δ= 7.48-7.37 (m, 3H, H_i), 7.35 (dd, J= 0.8 and 1.9 Hz, 1H, H_a), 6.30 (dd, J= 1.9 and 3 Hz, 1H, H_b), 6.05 (dd, J= 0.9 and 3 Hz, 1H, H_c), 5.23 (s, 2H, H_f), 4.62 (s, 2H, H_h), 4.56 (s, 2H, H_g), 2.95 (t, J= 7.45 Hz, 2H, H_d), 2.72 ppm (t, J= 7.45 Hz, 2H, H_e). ^{13}C NMR: (75 MHz, CD_3CN, 298 K): δ= 172.98 (C_o), 155.37 (C_p), 142.34 (C_a), 140.22 (C_n), 137.69 (C_l), 136.43 (C_m), 132.19 (C_i), 131.27 (C_k), 130.51 (C_j), 111.33 (C_b), 106.26 (C_c), 63.87 (C_f), 33.77 (C_g), 33.18 (C_e), 31.34 (C_h), 23.96 ppm (C_d). FTIR (ATR, cm^{-1}): 3151, 3112, 3041, 2922, 1723, 1593, 1506, 1387, 1356, 1302, 1185, 1161, 1079, 1000, 913, 835, 801, 721, 654, 598. Elemental analysis calcd for $C_{16}H_{16}Br_2O_3$: C 46.18, H 3.88, found: C 46.23, H 3.88.

CBPQT^{4+}-Fu A solution of compound **2** (1.33 g, 3.21 mmol), compound **3** (2.26 g, 3.21 mmol) and naphthalene template (3.5 g, 9.62 mmol) in dry DMF (100 mL) was stirred under N_2 at room temperature for 10 days. The solvent was removed under vacuum and the residue was subjected to liquid-liquid extraction ($CHCl_3$/H_2O) to remove the naphthalene template. The aqueous layer was concentrated and the residue was purified using column chromatography (SiO_2: NH_4Cl(2M)/MeOH/$MeNO_2$, 4:4:2). All fractions containing the product were combined together and concentrated under vacuum. The residue was dissolved in a small amount of hot water and a saturated aqueous NH_4PF_6 solution was added to obtain **CBPQT^{4+}-Fu**, **4 PF_6^-**. The precipitate was collected by filtration, washed with water (×5), with CH_2Cl_2 (×3) and with Et_2O (×3) and dried under vacuum at 70 °C. To change the nature of the counterion of **CBPQT^{4+}-Fu** from **PF_6^-** to **Cl^-**, **CBPQT^{4+}-Fu**, **4 PF_6^-** was dissolved in a small amount of hot nitromethane and a saturated solution of tetraethylammonium chloride in nitromethane was added to obtain **CBPQT^{4+}-Fu**, **4 Cl^-**. The precipitate was collected by filtration, washed with nitromethane (×5), with CH_2Cl_2 (×3) and with Et_2O (×3) and dried under vacuum at 70 °C to obtain the desired product as a yellow powder (0.784 g, 9.63×10^{-1} mmol, 30% yield). ^{1}H NMR: (D_2O, 300 MHz, 298 K): δ= 9.28 (m, 4H, $H_{α1, α'1}$), 9.15 (m, 4H, $H_{α2, α'2}$), 8.35 (d, J= 6.5 Hz, 2H, $H_{β1}$), 8.25 (m, 4H, $H_{β'1, β2}$), 8.14 (d, J= 6.5 Hz, 2H, $H_{β'2}$), 8.0 (m, 2H, $H_{Ph2, Ph3}$), 7.9 (m, 1H, H_{Ph4}), 7.8 (m, 4H, H_{Ph1}), 6.07 (s, 2H, H_{g1}), 5.97 (s, 2H, H_{g3}), 5.93 (s, 2H, H_{g4}), 5.86 (s, 2H, H_{g2}), 5.45 (s, 2H, H_f), 4.77 (d, J= 1.2 Hz, 1H, H_a), 4.64 (dd, J = 3.2 Hz and 1.2 Hz, 1H, H_b), 2.14 (d, J= 3.2 Hz, 1H, H_c), 2.08 (t, J = 7.3 Hz, 2H, H_d), 1.89 ppm (m, 2H, H_e), ^{13}C NMR: (D_2O, 75 MHz, 298 K): δ= 173.81 (C_{10}), 152.75 (C_{11}), 148.56 (C_9), 147.77 (C_5), 144.72 (C_4), 147.34 (C_8), 145.75 , 144.96 , 144.93 , 144.73 , 141.18 (C_a), 136.93 (C_1), 136.81 (C_2), 136.44 (C_3), 135.95 (C_7), 135.54 (C_8), 135.03 (C_{Ph2}), 133.61(C_{Ph3}), 130.50 (C_{Ph4}), 130.26 (C_{Ph1}), 126.99 ($C_{β'1}$), 126.72 ($C_{β1}$), 126.43 ($C_{β2}$), 126.17 ($C_{β'2}$), 109.25 (C_b), 103.56 (C_c), 65.0 (C_{g2}), 64.80 (C_{g3}), 64.77 (C_{g4}), 63.49 (C_f), 61.88 (C_{g1}), 32.58 (C_e), 22.06 ppm (C_d). FTIR (ATR, cm^{-1}): 3362, 3120, 3042, 1731, 1634, 1561, 1508, 1447, 1359, 1281, 1229, 1160, 861, 786. HRMS: m/z calcd for $C_{44}H_{40}Cl_4N_4O_3$ + Na^+: 837.1723 [*M* + Na]$^+$; found: 837.1724

Napht-2 A solution of a naphthalene functionalized RAFT agent (**NaphtOH-CTA**)[48](112 mg, 1.96×10^{-1} mmol), AIBN (8 mg, 4.91×10^{-2} mmol), NIPAm monomer (2 g, 17.67 mmol) and DMAc monomer (195 mg, 1.96 mmol) in DMF (4 mL) was deoxygenated by bubbling nitrogen for 15 min at room temperature. The reaction flask was placed in an oil bath at 80 °C. The polymerization was allowed to proceed for 1 h under magnetic stirring. Then, the solution was cooled down with an ice bath and the copolymer was isolated by precipitation in *n*-hexane. The copolymer was isolated as a white powder (1.9 g, 1.61×10^{-1} mmol, 87wt% yield) after two successive precipitations from acetone into Et_2O and dried under vacuum.

Supporting Information

Full experimental details on compounds characterization, kinetic experiments, determination of the equilibrium constant K_{in}, and computational investigations are provided the Supporting Information.The authors have cited additional references within

The authors have cited an additional reference within the Supporting Information.[51]

Acknowledgements

These authors contributed equally to this work. We thank Dr. Laurent Bouteiller for his help concerning the characterization of host-guest complexes by ITC. PW thanks Joëlle Thuriot for the elemental analysis. This research was supported by the ANR agency (MISMATCH project, ANR-12-BS08-0005). The Chevreul Institute is thanked for its help in the development of this work through the ARCHI-CM project supported by the "Ministère de l'Enseignement Supérieur de la Recherche et de l'Innovation", the region "Hauts-de-France", the ERDF program of the European Union and the "Métropole Européenne de Lille". GC thanks the EPSRC (EP/E036244/1).

Keywords: chemical reactivity, Diels-Alder reaction, topological chemistry, supramolecular chemistry, host-guest chemistry

[1] J. Z. Zhang, S. Mehta, J. Zhang, *Trends Pharmacol. Sci.* **2021**, *42*, 845–856.

[2] J. C. Iovine, S. M. Claypool, N. N. Alder, *Trends Biochem. Sci.* **2021**, *46*, 902–917.

[3] A. A. Gavrilov, S. V. Razin, *Mol. Biol.* **2015**, *49*, 21–39.

[4] M. Montal, *Annu. Rev. Biophys. Biomol. Struct.* **1995**, *24*, 31–57.

[5] B. Alberts, A. Johnson, J. Lewis, M. Raff, K. Roberts, P. Walter, *Molecular Biology of the Cell*, W.W. Norton & Company, **2007**.

[6] T. Pan, T. Sosnick, *Annu. Rev. Biophys. Biomol. Struct.* **2006**, *35*, 161–175.
[7] P. J. Horn, C. L. Peterson, *Science* **2002**, *297*, 1824–1827.
[8] J. E. Johnson, *Curr. Opin. Struct. Biol.* **2010**, *20*, 210–216.
[9] M. G. Mateu, *Arch. Biochem. Biophys.* **2013**, *531*, 65–79.
[10] B. Städler, A. D. Price, R. Chandrawati, L. Hosta-Rigau, A. N. Zelikin, F. Caruso, *Nanoscale* **2009**, *1*, 68–73.
[11] F. Hof, J. Rebek, *Proc. Natl. Acad. Sci.* **2002**, *99*, 4775–4777.
[12] J. Rebek, *Acc. Chem. Res.* **2009**, *42*, 1660–1668.
[13] M. D. Pluth, R. G. Bergman, K. N. Raymond, *J. Am. Chem. Soc.* **2008**, *130*, 11423–11429.
[14] M. D. Pluth, D. Fiedler, J. S. Mugridge, R. G. Bergman, K. N. Raymond, *Proc. Natl. Acad. Sci.* **2009**, *106*, 10438–10443.
[15] Y. R. Hristova, M. M. J. Smulders, J. K. Clegg, B. Breiner, J. R. Nitschke, *Chem Sci* **2011**, *2*, 638–641.
[16] S. Liu, B. C. Gibb, *Chem. Commun.* **2011**, *47*, 3574–3576.
[17] R. Custelcean, J. Bosano, P. V. Bonnesen, V. Kertesz, B. P. Hay, *Angew. Chem. Int. Ed.* **2009**, *48*, 4025–4029.
[18] O. Diels, K. Alder, *Justus Liebigs Ann. Chem.* **1928**, *460*, 98–122.
[19] T. Murase, S. Horiuchi, M. Fujita, *J. Am. Chem. Soc.* **2010**, *132*, 2866–2867.
[20] M. Yoshizawa, M. Tamura, M. Fujita, *Science* **2006**, *312*, 251–254.
[21] K. Ikemoto, Y. Inokuma, M. Fujita, *J. Am. Chem. Soc.* **2011**, *133*, 16806–16808.
[22] Y. Inokuma, S. Yoshioka, M. Fujita, *Angew. Chem. Int. Ed.* **2010**, *49*, 8912–8914.
[23] J. B. Siegel, A. Zanghellini, H. M. Lovick, G. Kiss, A. R. Lambert, J. L. St.Clair, J. L. Gallaher, D. Hilvert, M. H. Gelb, B. L. Stoddard, K. N. Houk, F. E. Michael, D. Baker, *Science* **2010**, *329*, 309–313.
[24] A. Palma, M. Artelsmair, G. Wu, X. Lu, S. J. Barrow, N. Uddin, E. Rosta, E. Masson, O. A. Scherman, *Angew. Chem. Int. Ed.* **2017**, *56*, 15688–15692.
[25] M. M. J. Smulders, J. R. Nitschke, *Chem Sci* **2012**, *3*, 785–788.
[26] L. S. Mizoue, W. J. Chazin, *Curr. Opin. Struct. Biol.* **2002**, *12*, 459–463.
[27] D. P. Goldenberg, T. E. Creighton, *Biopolymers* **1985**, *24*, 167–182.
[28] K. G. Daniels, Y. Suo, T. G. Oas, *Proc. Natl. Acad. Sci.* **2015**, *112*, 9352–9357.
[29] T. Bordelon, S. K. Montegudo, S. Pakhomova, M. L. Oldham, M. E. Newcomer, *J. Biol. Chem.* **2004**, *279*, 43085–43091.
[30] D. Keramisanou, N. Biris, I. Gelis, G. Sianidis, S. Karamanou, A. Economou, C. G. Kalodimos, *Nat. Struct. Mol. Biol.* **2006**, *13*, 594–602.
[31] A. Mohan, C. J. Oldfield, P. Radivojac, V. Vacic, M. S. Cortese, A. K. Dunker, V. N. Uversky, *J. Mol. Biol.* **2006**, *362*, 1043–1059.
[32] S. Devarakonda, K. Gupta, M. J. Chalmers, J. F. Hunt, P. R. Griffin, G. D. Van Duyne, B. M. Spiegelman, *Proc. Natl. Acad. Sci.* **2011**, *108*, 18678–18683.
[33] D. D. Boehr, R. Nussinov, P. E. Wright, *Nat. Chem. Biol.* **2009**, *5*, 789–796.
[34] S. B. Hari, E. A. Merritt, D. J. Maly, *Chem. Biol.* **2014**, *21*, 628–635.
[35] J. Bigot, M. Bria, S. T. Caldwell, F. Cazaux, A. Cooper, B. Charleux, G. Cooke, B. Fitzpatrick, D. Fournier, J. Lyskawa, M. Nutley, F. Stoffelbach, P. Woisel, *Chem. Commun.* **2009**, 5266–5268.
[36] P. L. Anelli, P. R. Ashton, R. Ballardini, V. Balzani, M. Delgado, M. T. Gandolfi, T. T. Goodnow, A. E. Kaifer, D. Philp, M. Pietraszkiewicz, L. Prodi, M. V. Reddington, A. M. Z. Slawin, N. Spencer, J. F. Stoddart, C. Vicent, D. J. Williams, *J. Am. Chem. Soc.* **1992**, *114*, 193–218.
[37] M. Asakawa, W. Dehaen, G. L'abbé, S. Menzer, J. Nouwen, F. M. Raymo, J. F. Stoddart, D. J. Williams, *J. Org. Chem.* **1996**, *61*, 9591–9595.
[38] P. L. Anelli, P. R. Ashton, R. Ballardini, V. Balzani, M. Delgado, M. T. Gandolfi, T. T. Goodnow, A. E. Kaifer, D. Philp, *J. Am. Chem. Soc.* **1992**, *114*, 193–218.
[39] D. N. Tran, D. Colesnic, S. Adam de Beaumais, G. Pembouong, F. Portier, Á. A. Queijo, J. Vázquez Tato, Y. Zhang, M. Ménand, L. Bouteiller, M. Sollogoub, *Org Chem Front* **2014**, *1*, 703–706.
[40] L. S. Witus, K. J. Hartlieb, Y. Wang, A. Prokofjevs, M. Frasconi, J. C. Barnes, E. J. Dale, A. C. Fahrenbach, J. F. Stoddart, *Org. Biomol. Chem.* **2014**, *12*, 6089–6093.
[41] K. K. Park, Y. S. Kim, S. Y. Lee, H. E. Song, J. W. Park, *J. Chem. Soc. Perkin Trans. 2* **2001**, 2114–2118.
[42] D. Benitez, E. Tkatchouk, I. Yoon, J. F. Stoddart, W. A. I. Goddard, *J. Am. Chem. Soc.* **2008**, *130*, 14928–14929.
[43] M. Bria, G. Cooke, A. Cooper, J. F. Garety, S. G. Hewage, M. Nutley, G. Rabani, P. Woisel, *Tetrahedron Lett.* **2007**, *48*, 301–304.
[44] J. Bigot, D. Fournier, J. Lyskawa, T. Marmin, F. Cazaux, G. Cooke, P. Woisel, *Polym. Chem.* **2010**, *1*, 1024–1029.
[45] J. Carneiro de Oliveira, M.-P. Laborie, V. Roucoules, *Molecules* **2020**, *25*, 243–255.
[46] L. J. S. Witus, K. Hartlieb, Y. Wang, A. Prokofjevs, M. C. Frasconi, J. Barnes, J. Dale, C. A. Fahrenbach, J.F. Stoddart, *J. Org. Biomol. Chem*. **2014**, 12 (32), 6089–6093.
[47] P. L. Anelli, P.R. Ashton, R. Ballardini, V. Balzani, M. Delgado, M. T. Gandolfi, T. T. Goodnow, A. E. Kaifer, D. Philp, J. *Am. Chem. Soc*. **1992**, 114 (1), 193–218.
[48] A. Malfait, F. Coumes, D. Fournier, G. Cooke, P. Woisel, *Eur. Polym. J.* **2015**, 69, 552–558.
[49] G. Cooke, P.Woisel, M. Bria, F. Delattre, J. F. Garety, S. G. Hewage, G. Rabani, G. Rosair, *Org. Lett.* **2006**, 8 (7), 1423-1426
[50] M. Asakawa, W. Dehaen, G. L'abbé, S. Menzer, J. Nouwen, F. M. Raymo, J. F. Stoddart, D. J. Williams, *J. Org. Chem.* **1996**, 61 (26), 9591–9595.
[51] P.Thordarson, *Chem. Soc. Rev.* **2011**, 40 (3), 1305–1323.

Entry for the Table of Contents

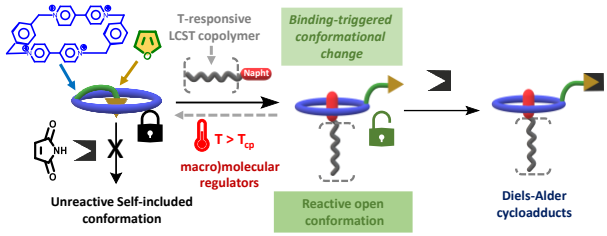

Combining two biorelevant concepts, *i.e.*, compartmentalization and regulator-induced conformational change allows controlling the Diels-Alder reactivity between a furan moiety and maleimide in water. Using a thermosensitive regulator enables the Diels-Alder reaction to be turned off at elevated temperature, whereas it is activated by lowering the temperature, representing a rare example of reduced reactivity at elevated temperature.